Dispersion-shaped ac Stark phase shift of Ca intercombination transitions with a time-domain atom interferometer

Tomoya Akatsuka,[*] Kazuya Tanihara, Kenji Komito, Kentaro Ooi, and Atsuo Morinaga[†]
Faculty of Science and Technology, Tokyo University of Science, Noda-shi, Chiba 278-8510, Japan
(Received 8 June 2012; published 28 August 2012)

A time-domain atom interferometer with a cold calcium atomic ensemble has been developed with a phase resolution $\sigma_\phi = 140/\sqrt{\tau}$ mrad/s$^{1/2}$ at the integration time τ. Using this atom interferometer, the dispersion-shaped ac Stark phase shift with a sharp reversal on resonance was demonstrated under the perturbation light near the resonance frequency of the $^1S_0$, $m_J = 0$ $-^3P_1$, $m_J = -1$ transition. The phase shift was well described by a convolution of functions of the ac Stark potential and a Rabi excitation, and it was found that the lifetime of the $^3P_1$ state is 0.45 $\pm$ 0.03 ms.

DOI: 10.1103/PhysRevA.86.023418 PACS number(s): 32.60.+i, 03.75.Dg, 37.10.Gh, 37.25.+k

I. INTRODUCTION

Atom interferometers are useful for various physics, such as the precise measurement of gravitational acceleration constant [1], the fundamental test of quantum physics [2], the measurement of atomic properties [3], and so on [4]. In the third case, Ramsey-Bordé interferometers [5], which are composed of two different internal states of atoms as two arms in an atom interferometer, are often used. The phases of these two states shift according to their respective perturbation, so that the phase of interference fringes shifts, similarly to a polarization interferometer in optics. When the two arms are irradiated with a laser field detuned far from the resonance frequency during the interrogation time, the interference fringes shift owing to the ac Stark effect, in proportion to laser intensity and in inverse proportion to detuning frequency [6]. These experiments were performed using space-domain atom interferometers with a thermal atomic beam [6–9] or time-domain atom interferometers with an ensemble of cold atoms [10]. In the former, phase shift occurs when atoms move in a gradient of an ac Stark potential [11]. On the other hand, in the latter, it occurs owing to the temporal variation of the applied scalar potential, which is called a scalar Aharonov-Bohm effect [12,13]. Therefore, phase shift is dispersive in the former and nondispersive in the latter. To determine the decay rate or lifetime of a state using a measured phase shift, a time-domain atom interferometer is suitable, because interference fringes in a space-domain atom interferometer disappear destructively with an increase in phase dispersion of more than π [14].

The measurement of an ac Stark phase shift on resonance should reveal a familiar dispersion-shaped dependence [15]. The dispersion-shaped frequency shift through resonance was measured previously using microwave spectroscopy of ground-state hyperfine transitions [16] and was used as dispersive signals for the frequency stabilization of lasers [17]. On the other hand, a dispersion-shaped phase shift of the ac Stark effect was first observed using an atom interferometer with guided-wave Bose-Einstein condensates by Deissler *et al.* [18], but with a broadened linewidth attributed to a collective light scattering effect. We intended to observe a dispersion-shaped phase shift with a sharp reversal on resonance using an accurate time-domain atom interferometer and to determine the lifetime of the metastable state.

A calcium atom interferometer is comprised of the $^3P_1$ metastable state and the ground $^1S_0$ state of calcium atom [19,20]. The frequency of the intercombination line between the $^3P_1$ and $^1S_0$ states is known with an uncertainty of only a few hertz [21,22]; however, the lifetimes of the $^3P_1$ state reported by many authors ranged from 0.33 to 0.57 ms, depending on the experimental method used to determine them [23]. Drozdowski *et al.* reported a lifetime of 0.34 $\pm$ 0.02 ms, determined by measuring the decay of the fluorescence from a thermal atomic beam excited selectively with a short-pulse dye laser [24], which is in agreement with the calculation employing the relativistic effective operator formalism [25]. However, Degenhardt *et al.* have reported a lifetime of 0.43 $\pm$ 0.01 ms, determined by measuring the fluorescence from cold ensembles after excitation with a π pulse [21]. Therefore, it is desired to examine the lifetime of the $^3P_1$ state from other measurements such as a dispersion-shaped phase shift.

In this paper, the authors demonstrate a dispersion-shaped ac Stark phase shift with a sharp reversal on resonance using a time-domain atom interferometer with a 10-mrad phase resolution. The lifetime of the $^3P_1$ state is deduced from the decay rate, which is obtained by fitting a phase-shift function for the ac Stark effect to the experimental one.

II. PHASE-SHIFT FUNCTION

The relevant energy levels for ^{40}Ca are depicted in Fig. 1. The magnetic field of 0.76 mT was applied during the interferometer measurement to split the $^3P_1$ state into the Zeeman sublevels m_J with the frequency shifts $m_j \times 16$ MHz. The resulting Zeeman shifts was much larger than the total transition linewidth of a few megahertz. The ground $4s^2\ ^1S_0$ state and metastable $4s4p\ ^3P_1$ and $m_J = 0$ ($^3P_{1,0}$) state were used to form a time-domain atom interferometer by exciting atoms with the π-polarized laser whose frequency was resonant to an intercombination transition $^1S_0$ $-^3P_{1,0}$ at a wavelength of 657 nm [20]. The ac Stark phase shift in the $^1S_0$ state was induced by applying a σ^--circularly polarized laser

[*]Present address: RIKEN, 2-1 Hirosawa Wako-shi, Saitama 351-0198, Japan.
[†]morinaga@ph.noda.tus.ac.jp

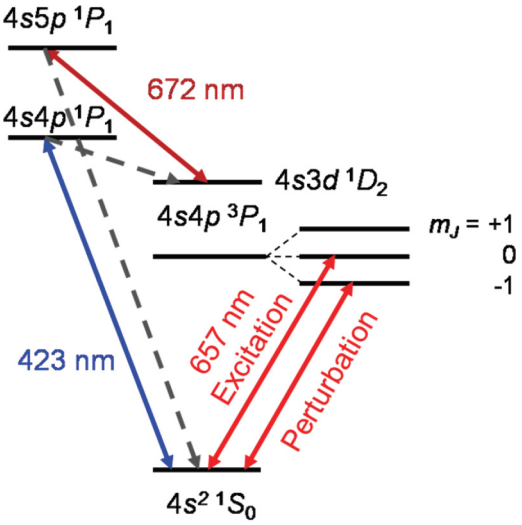

FIG. 1. (Color online) Partial energy level diagram of ^{40}Ca under a magnetic field of 0.76 mT, together with related transitions.

whose frequency was near the resonance of the $^1S_0 - {}^3P_{1,-1}$ transition on atoms.

Cold calcium atoms with a temperature of several millikelvins generate the Doppler width of a few megahertz in the resonance spectrum. When an atom moves with a velocity v along the propagation direction of the perturbation laser, the resonance frequency ω_v shifts from that of the atom at rest, due to the Doppler effect. If the frequency of the perturbation laser, ω, is tuned near the resonance frequency ω_v of the $^1S_0 - {}^3P_{1,-1}$ transition with a detuning frequency of $\omega - \omega_v$, the laser field causes an ac Stark potential [6,11] in the $^1S_0$ ground state given by

$$U = \frac{\hbar(\omega - \omega_v)}{2} \frac{3I\lambda^3/(\pi hc\gamma)}{3I\lambda^3/(\pi hc\gamma) + 1 + [2(\omega - \omega_v)/\gamma]^2}, \quad (1)$$

where I is the laser intensity, γ is the decay rate from the $^3P_1$ state, λ is the wavelength, h is Planck's constant, $\hbar$ is h divided by 2π and c is the speed of light in vacuum. Here only one transition is being considered. The ac Stark potential is applied to the atom during a duration t_p. Then, the phase of atoms in the $^1S_0$ state with a velocity v shifts by $\Delta\phi_{ac} = U(\omega - \omega_v, \gamma)t_p/\hbar$ owing to the scalar Aharonov-Bohm effect [12,13]. The velocities of atoms, which are involved in the interference, are selected from the width of the Rabi-excitation pulse of the $^1S_0 - {}^3P_{1,0}$ transition, because its width is smaller than the Doppler width. The Rabi-excitation probability with a π pulse area at a pulse duration T is given by [26]

$$P(\omega_v) = \left[\frac{1/T}{\omega_v^2 + (\pi/T)^2}\right] \sin^2\left[\frac{\sqrt{\omega_v^2 + (\pi/T)^2}}{2} T\right]. \quad (2)$$

Therefore, the phase-shift function is given by a convolution of Eqs. (1) and (2), as

$$\phi(\omega) = \int_{-\infty}^{\infty} U(\omega - \omega_v, \gamma)(t_p/\hbar)P(\omega_v)d\omega_v \Big/ \int_{-\infty}^{\infty} P(\omega_v)d\omega_v. \quad (3)$$

By comparing Eq. (3) with the experimental results, we can deduce the decay rate γ, i.e., the lifetime of the $^3P_1$ state.

III. EXPERIMENT

The present experimental procedures are shown in Fig. 2. First, we explain our procedure for a cold ensemble of Ca atoms in a magnetooptical trap (MOT). The used transitions are also shown in Fig. 1. The $^1S_0$–$4s4p\ ^1P_1$ transition at 423 nm with a natural linewidth of 34 MHz was used to trap a cold Ca atomic ensemble in a magnetooptical trap. The $4s3d\ ^1D_2$–$4s5p\ ^1P_1$ transition at 672 nm was used to return atoms in the $^1D_2$ state, which were decayed from the $4s4p\ ^1P_1$ excited state with a branching ratio of 10^{-5}, to the $^1S_0$ ground state via a higher $4s5p\ ^1P_1$ state [27].

The laser with a wavelength of 423 nm was based on a tapered-amplifier diode laser and a second harmonic generation (SHG) system. An amplified laser power of 350 mW at 846 nm was injected into a bowtie cavity with a periodically poled $KTiOPO_4$ (KTP) crystal [28] to obtain 40 mW at 423 nm. The cavity length was controlled by a piezoelectric transducer (PZT) and stabilized to the cavity resonance by the Hänsch-Couillaud technique [29]. The laser frequency was stabilized to a saturated absorption spectrum of the $^1S_0$–$^1P_1$ transition of Ca atoms in a discharge cell observed by the frequency modulation technique [30]. The output beam from the SHG cavity was divided into three parts: a slowing beam, MOT beams, and a probe beam. These outputs were switched on and off, and frequencies were shifted by individual acoustooptic modulators (AOMs) to set their detuning from the $^1S_0$–$^1P_{1,0}$ transition to -143, -33, and -33 MHz, respectively.

A Ca atomic beam from an oven at a temperature of 1088 K was decelerated by a counterpropagating slowing beam of 5 mW; then atoms were loaded to the MOT consisting of six orthogonal circularly polarized MOT beams and a quadrupole magnetic field. The beam powers and the magnetic field gradients in the trap region along the vertical and horizontal axes were 1 and 2 mW, and 0.8 and 0.4 mT/mm, respectively. The probe beam was set incident to atoms along the horizontal axis after turning off the MOT to evaluate the

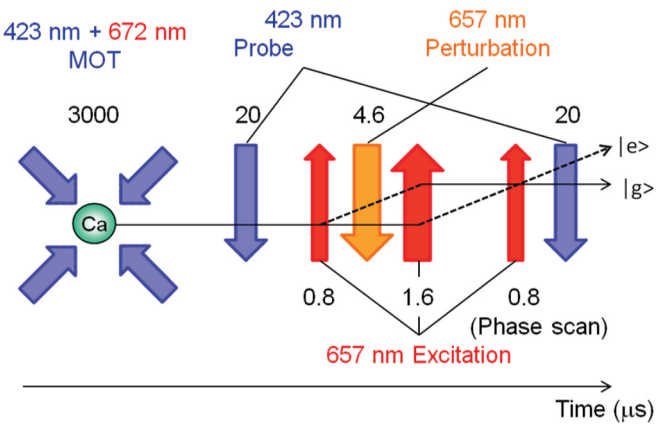

FIG. 2. (Color online) Experimental procedures. Numbers indicate time durations in μs. Ca atoms are cooled and trapped during 3 ms in the magnetooptical trap (MOT). After a release of cold atoms from the MOT, three 657-nm pulses of $\pi/2$, π, and $\pi/2$ (0.8, 1.6, and 0.8 μs) irradiated to atoms make an atom interferometer. A perturbation pulse with duration of 4.6 μs was inserted between the first $\pi/2$ and π pulses. The probability of atoms in the excited state was measured by two probe pulses with a duration of 20 μs.

atomic population in the $^1S_0$ ground state by measuring the fluorescence intensity using a photomultiplier tube (PMT). Typically, 10^5 atoms were trapped every 3.2 ms. From the trap lifetime of 20–40 ms, we estimated that about 85% − 90% of the atoms used for the measurement were recaptured in the present MOT. This cycle time was optimized as short as possible in a range in which the number of trapped atoms did not decrease significantly, so as to improve the signal-to-noise ratio of the interference fringes by increasing the number of measurements in unit time.

The laser system operating at 657 nm with a linewidth of a few hertz has been described in detail in an earlier publication [9]. The laser beam was divided into two parts: an excitation beam for the atom interferometer in the $^1S_0 - ^3P_{1,0}$ transition and a perturbation beam scanned around the resonance of the $^1S_0 - ^3P_{1,-1}$ transition, both of which were power amplified up to 30 mW at its maximum by injection locking two individual antireflection (AR)-coated diode lasers to them. The perturbation beam was frequency offset by −16 MHz from the excitation beam, which was resonant to the $^1S_0 - ^3P_{1,0}$ transition under the bias magnetic field of 0.76 mT. Both beams were mode cleaned to nearly perfect Gaussian beam profiles using pinholes.

A time-domain atom interferometer was constituted with cold atomic clouds released from the MOT. First, cold atoms were accumulated in the MOT for 3 ms with lasers at 423 and 672 nm. At 100 μs after turning off the laser light and the magnetic field for the MOT, the homogeneous bias magnetic field of 0.76 mT was applied on atoms along the vertical axis, to split the Zeeman sublevels of the $^3P_1$ state. The excitation beam with polarization parallel to the magnetic field was incident to atoms antiparallel to the 423-nm probe beam. The beam radius of 1.1 mm was about twofold larger than that of atomic clouds of 130 μs after turning off the MOT. The beam power of 4.8 mW was adjusted to be a π-pulse area for Rabi excitation at pulse duration of 1.6 μs. A typical spectrum of the $^1S_0 - ^3P_{1,0}$ transition showed a Doppler broadening of 4.3 MHz due to the residual velocity distribution, from which we found that the atom temperature was 7 mK [see Fig. 5(a)].

To compose an atom interferometer, the pulses of the 657-nm excitation beam with pulse areas of $\pi/2$, π, and $\pi/2$ were sequentially irradiated on the atoms with pulse separations of 5 μs. To observe interference fringes, the laser phase $\Delta\phi_L$ of the third pulse was scanned by modulating the phase of the rf signal driving the AOM. Two 423-nm probe pulses with a width of 20 μs were irradiated before and after the 657-nm excitation pulse trains, and the number of atoms in the $^1S_0$ ground state was measured by monitoring the fluorescent signal from the $^1P_1$ state. We obtained the total number of atoms in the MOT at the first probe pulse and the number of atoms left in the $^1S_0$ state after excitations at the second probe pulse, respectively. Using them, we calculated the fraction of the number of atoms excited to the $^3P_1$ state.

IV. RESULTS AND DISCUSSIONS

To obtain the interference fringes as a time series, the laser phase was scanned from 0 to 3π rad in 30 steps. The 100 measurements of the interference fringes were accumulated repeatedly every 9.6 s. Each fringe pattern was fitted by a sine function to obtain the phase data. The Allan deviation calculated from the phase data in an operation of 5000 s is shown in Fig. 3, which indicates the phase resolution of the atom interferometer as a function of the average time. The Allan deviation decreased with $\sigma_\phi = 140/\sqrt{\tau}$ mrad/s$^{1/2}$ and reached 4.5 mrad at an integration time $\tau = 1000$ s. However, this value was two orders larger than the shot noise limit estimated from the present fluorescence photons, the detection efficiency, and the visibility of fringes. Probably it will depend on the power fluctuation of the 423-nm probe laser. Figure 4 shows a typical interference fringe with an integration of 5000 s, which corresponds to a phase resolution of 2 mrad. The visibility of the fringe was restricted to 0.18, due to the temperature of the present cold atoms.

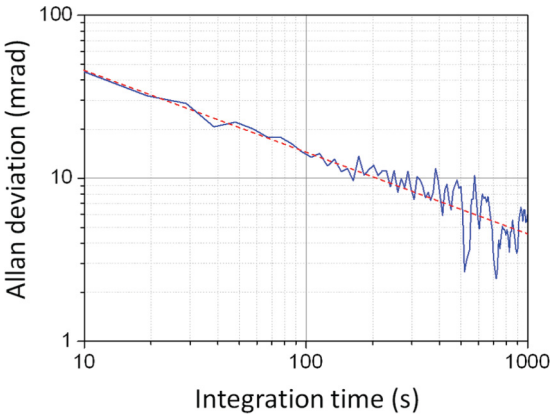

FIG. 3. (Color online) Allan deviation of phase versus averaging time in a time-domain atom interferometer.

The perturbation beam was incident to atoms in the same path of the excitation beam with the polarization perpendicular to the magnetic field, containing equal $\sigma^{\pm}$ polarization components. The AOM of the perturbation beam was utilized to scan the laser frequency around the resonance of the $^1S_0 - ^3P_{1,-1}$ transition and to apply the pulse modulation on the beam. A typical spectrum is shown in Fig. 5(a). The beam radius of 1.45 mm was about three times larger than that of atomic clouds. A total beam power of 5.2 mW resulted in

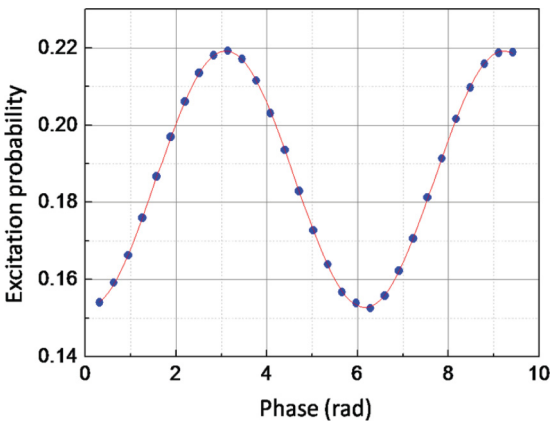

FIG. 4. (Color online) Typical interference fringes integrated for 170 s per phase step, together with a sine function fitted to the data. The standard deviation of the residuals divided by the amplitude of the sine was 0.005.

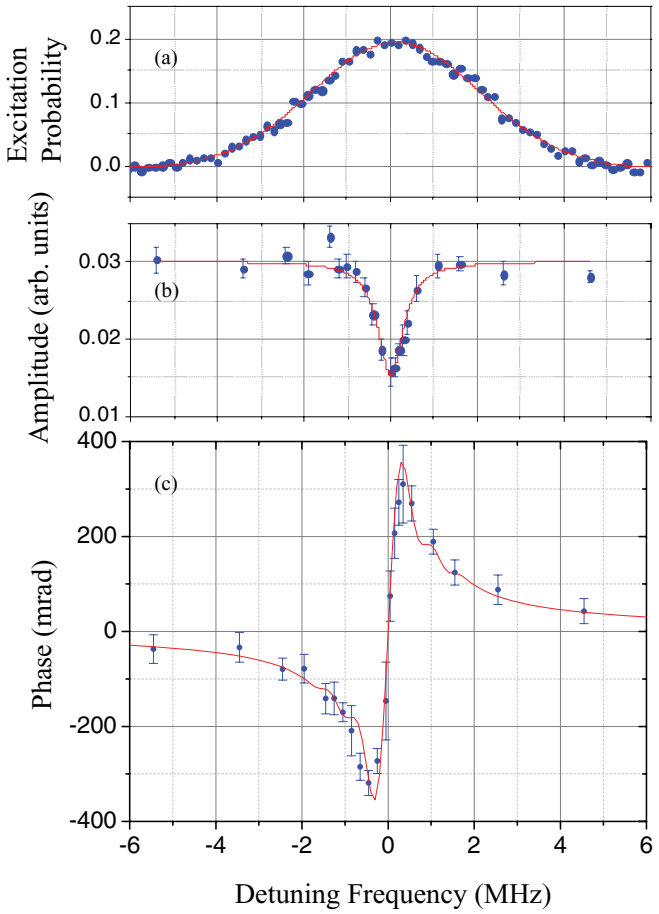

FIG. 5. (Color online) (a) Probability excited by a Rabi pulse versus detuning frequency of perturbing laser from the resonance between the $^1S_0$ and $^3P_{1,-1}$ states. Solid line is a Gauss profile. (b) Amplitude of interference signal versus detuning frequency. Solid line is a Lorentz curve. (c) Phase of interference versus detuning frequency of perturbing laser. Solid line is a curve calculated using Eq. (3) with $I = 71$ mW/cm^2 and $\gamma = 2.18 \times 10^3$ s^{-1}.

an average laser intensity of 71 ± 4 mW/cm^2 over atoms for the σ^- polarization light. The uncertainty of the intensity comes mainly from uncertainties of the measurements of the absolute power and the beam diameter. The perturbation beam was irradiated for $t_p = 4.6$ μs between the first and second excitation pulses, in which atoms were in the superposition state of $^1S_0$ and $^3P_{1,0}$; thus, a phase shift was induced by the difference between the ac Stark potentials in the two states.

Interference fringes with a perturbation pulse at several detuning frequencies were observed at an average time of 200 s. Figures 5(b) and 5(c) show the measured amplitude of fringes and the phase shift of interference fringes as functions of the detuning frequency of the perturbation pulse, respectively. On resonance, most of the atoms, which are excited to the $^3P_{1,-1}$ state from the ground $^1S_0$ state by the perturbation pulse, remain there during the entire interferometer measurement, so that they do not contribute to the interference. By this process, the amplitude of the interference signal on resonance decreased to half that without perturbation. Furthermore, only atoms with a Doppler shift within a resonance linewidth of the Rabi-excitation pulse contributed to the interference signal. This was confirmed from the fact that the observed dip width (FWHM = 700 kHz) was somewhat wider than the linewidth of the Rabi-excitation pulse (FWHM $\approx$ 550 kHz). On the other hand, we observed a dispersion-shaped phase shift with a sharp reversal on resonance, where the uncertainty of the phase was about 80 mrad. The experimental data were compared with the result of a calculation using Eq. (3) with Eqs. (1) and (2), and the laser intensity $I = 71$ mW/cm^2. By fitting only the parameter γ to the experimental data, the amplitude and shape of the phase shifts agree well with the experimental ones within uncertainties of the data, as shown in Fig. 5(c), reproducing fine structures due to the Rabi oscillation. The decay rate of the $^3P_1$ state was evaluated to be $\gamma = (2.18 \pm 0.10) \times 10^3$ s^{-1} by the χ^2 test. The uncertainty is statistical and will be smaller for a longer integration time.

We shall discuss the contribution from other transitions to the ac Stark phase shift. The $^1S_0 - ^3P_{1,1}$ transition is coupled with the σ^+ polarization component of the perturbation beam with a detuning of approximately 32 MHz, which caused a phase shift of 7 mrad with a frequency dependence of -0.2/mrad/MHz. In Fig. 5(c), this systematic shift subtracted from the experimental data. The influence of the $^1S_0$–$^1P_1$ transition at 423 nm was less than 0.02 mrad. Thus, contributions from other transitions to the phase shift were negligible small.

The present Doppler broadening was about one order wider than the Rabi broadening, as shown in Figs. 5(a) and 5(b). The width of the curve in Fig. 5(c) is set mostly by the Rabi broadening. It means that the smaller line-broadening effects, such as inhomogeneity of magnetic field, collisions and so on, should be negligible, even if the broadening is large compared to the natural linewidth. It also means that the dispersion curve does not much depend on the fluctuation of the Doppler profile due to the atomic temperature. The fluctuation of the atomic temperature will also cause the changes of the number of atoms and the spread of atomic ensemble. However, the former was already excluded from the uncertainty of the probability by the probe method used and the latter was negligible compared with the statistical uncertainty. Finally, taking the uncertainty of the perturbation laser intensity $I = 71 \pm 4$ mW/cm^2 into account, we concluded that the decay rate of the $^3P_1$ state is $\gamma = (2.18 \pm 0.15) \times 10^3$ s^{-1}.

From the above result, the lifetime of the $^3P_1$ state is deduced to be 0.45 ± 0.03 ms, which is in good agreement with that obtained by Degenhardt *et al.* [21]. The present uncertainty was three times that of the latter. However, the uncertainty will be improved if we enlarge a visibility of the interference fringes using a sub-Doppler cooling [31] and/or if we measure the phase during a longer integration time and the laser intensity with higher accuracy. The present method will be superior to the fluorescence method, which is hampered by fluorescence from other transitions [24]. Thus, we presented a method to measure a lifetime of a state using an atom interferometer.

V. CONCLUSION

In conclusion, we developed a time-domain atom interferometer using cold calcium atoms with a phase resolution $\sigma_\phi = 140/\sqrt{\tau}$ mrad/s$^{1/2}$ at the integration time τ. Using this

atom interferometer, we measured the phase shift due to the ac Stark effect of the perturbed laser through the resonance of the $^1S_0 - {}^3P_{1,-1}$ intercombination transition. We demonstrated the dispersion-shaped ac Stark phase shift with a sharp reversal on resonance. The experimental data were well described by a theoretical dispersion-shaped function and the lifetime of the $^3P_1$ state was deduced to be 0.45 ± 0.03 ms. The present result confirms the lifetime of the $^3P_1$ state measured by the emitted fluorescence photons from an ensemble of ultracold Ca atoms excited by a π pulse at 657 nm [21].

ACKNOWLEDGMENTS

We are indebted to Osamu Naganuma, Hiromi Iwase, Taku Kumiya, and Dr. Kazuhito Honda for producing a 423-nm laser and Norihiro Tanabe and Yudai Kannno for producing the MOT. This research was partially supported by Grant-in-Aid for Scientific Research on Innovative Areas "Extreme quantum world opened up by atoms" (Grant No. 21104006) from the Ministry of Education, Culture, Sports, Science, and Technology, Japan.

[1] A. Peters, K. Y. Chung, and S. Chu, Metrologia **38**, 25 (2001).
[2] S. Durr, T. Nonn, and G. Rempe, Nature **395**, 33 (1998).
[3] C. R. Ekstrom, J. Schmiedmayer, M. S. Chapman, T. D. Hammond, and D. E. Pritchard, Phys. Rev. A **51**, 3883 (1995).
[4] A. D. Cronin, J. Schmiedmayer, and D. E. Pritchard, Rev. Mod. Phys. **81**, 1051 (2009).
[5] Ch. J. Bordé, Phys. Lett. **140**, 10 (1989).
[6] U. Sterr, K. Sengstock, J. H. Müller, D. Bettermann, and W. Ertmer, Appl. Phys. B **54**, 341 (1992).
[7] F. Riehle, A. Witte, Th. Kisters, and J. Helmcke, Appl. Phys. B **54**, 333 (1992).
[8] A. Morinaga, T. Tako, and N. Ito, Phys. Rev. A **48**, 1364 (1993).
[9] T. Akatsuka, Y. Mori, N. Sone, Y. Ohtake, M. Machiya, and A. Morinaga, Phys. Rev. A **84**, 023633 (2011).
[10] K. Sengstock, U. Sterr, G. Hennig, D. Bettermann, J. H. Müller, and W. Ertmer, Opt. Commun. **103**, 73 (1993).
[11] J. Dalibard and C. Cohen-Tannoudji, J. Opt. Soc. Am. B **2**, 1707 (1985).
[12] Y. Aharonov and D. Bohm, Phys. Rev. **115**, 485 (1959).
[13] B. E. Allman, A. Cimmino, A. G. Klein, G. I. Opat, H. Kaiser, and S. A. Werner, Phys. Rev. Lett. **68**, 2409 (1992).
[14] K. Numazaki, H. Imai, and A. Morinaga, Phys. Rev. A **81**, 032124 (2010).
[15] A. Kastler, J. Opt. Soc. Am. **53**, 902 (1963).
[16] A. M. Bonch-Bruevich and V. A. Khodovoi, Usp. Fiz. Nauk **93**, 71 (1967) [Sov. Phys. Usp. **10**, 637 (1968)].
[17] R. L. Barger and J. L. Hall, Phys. Rev. Lett. **22**, 4 (1969).
[18] B. Deissler, K. J. Hughes, J. H. T. Burke, and C. A. Sackett, Phys. Rev. A **77**, 031604(R) (2008).
[19] A. Morinaga, M. Nakamura, T. Kurosu, and N. Ito, Phys. Rev. A **54**, R21 (1996).
[20] T. Trebst, T. Binnewies, J. Helmcke, and F. Riehle, IEEE Trans. Instrum. Meas. **48**, 535 (2001).
[21] C. Degenhardt, H. Stoehr, C. Lisdat, G. Wilpers, H. Schnatz, B. Lipphardt, T. Nazarova, P.-E. Pottie, U. Sterr, J. Helmcke, and F. Riehle, Phys. Rev. A **72**, 062111 (2005).
[22] U. Sterr, C. Degenhardt, H. Stoehr, C. Lisdat, H. Schnatz, J. Helmcke, F. Riehle, G. Wilpers, C. W. Oates, and L. Hollberg, C. R. Phys. **5**, 845 (2004).
[23] R. Drozdowski, J. Kwela, and M. Walkiewicz, Z. Phys. D **27**, 321 (1993).
[24] R. Drozdowski, M. Ignaciuk, J. Kwela, and J. Heldt, Z. Phys. D **41**, 125 (1997).
[25] E. Luc-Koening, J. Phys. B **14**, 1052 (1974).
[26] J. Vanier and C. Audoin, *The Quantum Physics of Atomic Frequency Standards* (Adam Hilger, Bristol and Philadelphia, 1989).
[27] N. Beverini, F. Giammanco, E. Maccioni, F. Strumia, and G. Vissani, J. Opt. Soc. Am. B **6**, 2188 (1989).
[28] M. Pierrou, F. Laurell, H. Karlsson, T. Kellner, C. Czeranowsky, and G. Huber, Opt. Lett. **24**, 205 (1999).
[29] T. W. Hänsch and B. Couillaud, Opt. Commun. **35**, 441 (1980).
[30] T. Ikegami, S. Ohshima, and M. Ohtsu, Jpn. J. Appl. Phys. **28**, L1839 (1989).
[31] E. A. Curtis, C. W. Oates, and L. Hollberg, Phys. Rev. A **64**, 031403(R) (2001).